

# Optimized pap-smear image enhancement: hybrid Perona-Malik diffusion filter-CLAHE using spider monkey optimization

Ach Khozaimi<sup>1,2</sup>, Isnani Darti<sup>1</sup>, Wuryansari Muharini Kusumawinahyu<sup>1</sup>, Syaiful Anam<sup>1</sup>

<sup>1</sup>Department of Mathematics, Faculty of Mathematics and Natural Sciences, Brawijaya University, Malang, Indonesia

<sup>2</sup>Department of Computer Science, Trunojoyo University of Madura, Bangkalan, Indonesia

## Article Info

### Article history:

Received Jan 8, 2025

Revised Jun 16, 2025

Accepted Jul 10, 2025

### Keywords:

BRISQUE

Contrast enhancement-based image quality

CLAHE

Pap-smear

Perona-Malik diffusion filter

Spider monkey optimization

## ABSTRACT

Pap-smear image quality is crucial for cervical cancer detection. This study introduces an optimized hybrid approach that combines the Perona-Malik diffusion (PMD) filter with contrast-limited adaptive histogram equalization (CLAHE) to enhance pap-smear image quality. The PMD filter reduces the image noise, whereas CLAHE improves the image contrast. The hybrid method was optimized using spider monkey optimization (SMO PMD-CLAHE). Blind/reference-less image spatial quality evaluator (BRISQUE) and contrast enhancement-based image quality (CEIQ) are the new objective functions for the PMD filter and CLAHE optimization, respectively. The simulations were conducted using the SIPaKMeD dataset. The results indicate that SMO outperforms state-of-the-art methods in optimizing the PMD filter and CLAHE. The proposed method achieved an average effective measure of enhancement (EME) of 5.45, root mean square (RMS) contrast of 60.45, Michelson's contrast (MC) of 0.995, and entropy of 6.80. This approach offers a new perspective for improving pap-smear image quality.

*This is an open access article under the [CC BY-SA](https://creativecommons.org/licenses/by-sa/4.0/) license.*



## Corresponding Author:

Isnani Darti

Department of Mathematics, Faculty of Mathematics and Natural Sciences, Brawijaya University

Veteran Street No. 12-16, Malang 65145, Indonesia

Email: isnanidarti@ub.ac.id

## 1. INTRODUCTION

Cancer continues to be a global health concern, with cervical cancer posing a significant health risk, especially in developing countries [1]. In 2020, Indonesia reported 36,633 cases of cervical cancer, trailing only breast cancer [2]. The Global Cancer Observatory predicted 570,000 new cases and 311,000 deaths globally in 2018 [3]. Approximately 90% of cervical cancer-related deaths occur in developing countries [4]. Efforts to reduce cervical cancer mortality include incorporating information technology and artificial intelligence into screening procedures [5]. Noise reduction and contrast enhancement enhance medical image quality classification [6]. The Perona-Malik diffusion (PMD) filter minimizes image noise and enhances image smoothness while retaining key details and edges [7]. PMD uses a modified Gaussian function to weigh each pixel value, with higher values at the center and lower values at the periphery [8]. Studies have shown that PMD filters extract and identify malignant tumors in medical images [9]. In addition, the PMD filter has improved the deep learning performance in cervical cancer classification [10]. However, the PMD filter performance relies on the fine-tuning of its parameters. Tsotsios and Petrou [11] chose the PMD filter parameter iteratively. The other research uses particle swarm optimization (PSO) to select PMD parameters and improve the PMD filter performance [12].

Contrast-limited adaptive histogram equalization (CLAHE) is a variant of adaptive histogram equalization (AHE) that limits contrast enhancement [13]. CLAHE effectively improves pap-smear images and enhances VGG16, InceptionV3, and EfficientNet performance in cervical cancer classification [14]. CLAHE has demonstrated effectiveness in enhancing image quality and improving the performance of various machine learning algorithms in cervical cancer classification tasks, including k-nearest neighbors (KNN) and artificial neural networks (ANN). Additionally, CLAHE has enhanced the detection accuracy of the you only look once (YOLO) algorithm in night-time road marking recognition, improved the performance of convolutional neural networks (CNNs) in lung cancer segmentation from computed tomography (CT) scan images, and contributed to water image classification tasks [15]–[19]. However, the effectiveness of CLAHE depends on its parameters, i.e., clip limit and tile size. Qassim *et al.* [16] set up a clip limit of 0.01 and a tile size of  $8 \times 8$  to get the best CLAHE performance, enhancing dental digital X-ray images. Several studies have applied different heuristic optimization algorithms to improve CLAHE performance.

PSO was used to optimize CLAHE performance with multi-objective functions, i.e., entropy and structure similarity index measure (SSIM). This approach maximized image contrast while minimizing distortion in X-ray medical images [17]. Fawzi *et al.* [18] applied the whale optimization algorithm (WOA) to optimize CLAHE performance with DataSignal as the objective function. The DataSignal results from multiplying the entropy by the peak signal-to-noise ratio (PSNR). It effectively enhances image contrast across datasets like faces-1999, BraTS, and Pasadena-houses 2000 [18]. The research in [19] employed the cuckoo search algorithm (CSA) with entropy and fast noise variance estimation (FNVE) as objective functions. This study showed superior performance in CLAHE optimization on the contrast enhancement evaluation 2016 (CEED2016) dataset compared to the bat firefly and flower pollination algorithms (FPA) [19]. In 2022, FPA optimized CLAHE with entropy and FNVE as objective functions. This study achieved notable noise reduction and contrast enhancement on the Pasadena-houses 2000 and diabetic retinopathy detection (DIARETDB0) datasets [20].

Surya and Muthukumaravel [21] used adaptive sailfish optimization (ASFO) to enhance CLAHE performance. This study focuses on maximizing contrast and entropy with successful enhancement outcomes on mammogram images from the mammographic image analysis society (MIAS) database [21]. Cat swarm optimization (CSO) is also used to enhance CLAHE performance with entropy and FNVE as objective functions. This approach outperformed traditional methods like hue, saturation, and lightness (HSL), European commission (EC), histogram equalization (HE), and CLAHE-CSA on the CEED2016 dataset [22]. In 2024, Haddadi *et al.* [23] introduced the pelican optimization algorithm (POA) to optimize CLAHE performance with several metrics, including PSNR, mean squared error (MSE), entropy, and SSIM as objective functions. This study uses a private dataset and outperforms the existing image enhancement techniques [23].

In this study, we aimed to enhance cervical image quality using a hybrid PMD filter-CLAHE. The PMD filter is used for noise reduction, and CLAHE is used for contrast enhancement. The spider monkey optimization (SMO) algorithm optimized the proposed method (hybrid PMD filter-CLAHE). SMO performs best in optimizing UCAV path-planning problems compared to other metaheuristic algorithms [24]. A new objective function was introduced in this study. The blind/reference-less image spatial quality evaluator (BRISQUE) is a new objective function for PMD filter optimization. BRISQUE is highly competitive with this no-reference image quality assessment (NR-IQA) approach. It is also statistically better than the popular full-reference image quality assessment (FR-IQA), such as PSNR and SSIM [25]. Contrast enhancement-based image quality (CEIQ) is a new objective function for CLAHE optimization. The CEIQ is computed using the histogram's characteristics of entropy, cross-entropy, and SSIM [26]. CEIQ identifies that the improved image exhibits contrast distortion [27].

This study used several metrics to evaluate the image denoising and contrast enhancement. MSE, SSIM, PSNR, CEIQ, entropy, enhancement measure estimation (EME), Michelson contrast (MC), and root mean square (RMS) contrast were used. These metrics evaluate image clarity, detail preservation, and contrast improvement. The proposed approach operates in the CIELAB color model of pap-smear images and offers several contributions.

First, hybrid SMO PMD-CLAHE provides the advantages of reducing noise and increasing contrast because most pap-smear images are noisy and have low contrast [28]. Second, BRISQUE and CEIQ are the new objective functions for the PMD filter and CLAHE optimization. BRISQUE was statistically better than PSNR and SSIM [25]. CEIQ can evaluate image contrast deformation [27]. Third, the SMO-PMD filter and SMO CLAHE outperformed state-of-the-art methods. This study offers a new perspective for improving cervical image quality and contributes to more accurate cervical cancer detection.

## 2. METHOD

Figure 1 illustrates the procedure for enhancing cervical images using a hybrid PMD filter-CLAHE optimized using the SMO algorithm. The input was a color image from the SIPaKMeD dataset. The SIPaKMeD dataset contains 4,049 annotated cervical cell images in five classes. Each class represents distinct morphological features vital for medical classification. Its primary characteristics include high variability in cell shapes, textures, noise, and contrast levels. This variability poses challenges in accurate classification [29]. The color image is split into lightness (L), green-red (A), and blue-yellow (B) color channels in the CIELAB color space. The CIELAB color space is designed to resemble the human visual system (HVS) [30]. Each channel underwent separate processing steps:

- Denoising: the A, B, and L channels are individually denoised using the SMO-PMD filter, which aims to reduce noise while preserving important image features such as edges;
- Contrast enhancement: after denoising, the L channel was further enhanced using SMO-CLAHE, which improved the local contrast and highlighted finer details.

Once all channels (L, A, and B) were processed (denoised and contrast-enhanced), they were recombined into the final enhanced pap-smear image. This enhanced image should exhibit an improved visual quality, reduced noise, and better contrast.

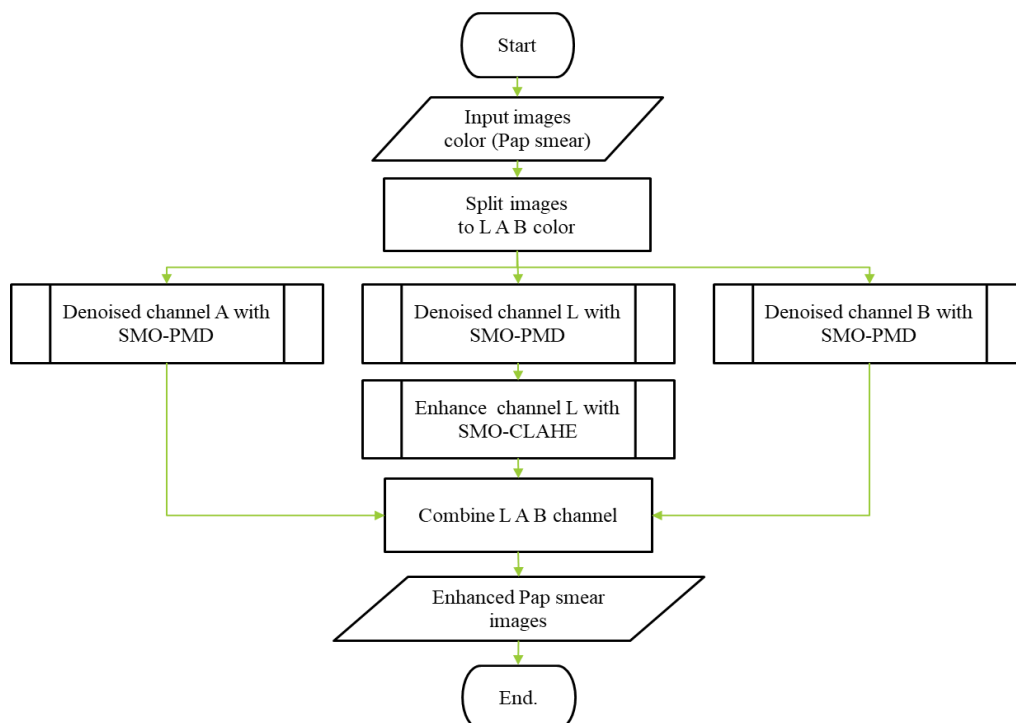


Figure 1. Flowchart of pap-smear image enhancement using SMO PMD filter-CLAHE

The hybrid PMD-CLAHE process was optimized using the SMO algorithm. The SMO optimizer was configured with 10 iterations and a population size of 50 to balance exploration and computational efficiency. The number of iterations (Niter) was set between 5 and 30 to control the degree of denoising. The diffusion coefficient ( $\kappa$ ) ranged from 10 to 100 to adjust the smoothing intensity, while the gradient threshold ( $\lambda$ ) was set between 0.1 and 0.25 to preserve image edges. The clip limit was set between 0.01 and 4 to manage contrast enhancement, and the tile size ranged from 2 to 16 to determine the local contrast regions. This configuration effectively balances the noise reduction and contrast enhancement.

### 2.1. Perona-Malik diffusion filter

A PMD filter was employed to minimize image noise while preserving the edges. This anisotropic diffusion process adjusts the diffusion coefficient according to the gradient of the image, thus facilitating edge-preserving smoothing [8]. Given an image  $I(x, y, t)$ , where  $x$  and  $y$  are spatial coordinates and  $t$  is the diffusion time (or iteration). The partial differential in (1) governed the evolution of the image under the PMD.

$$\frac{\partial I}{\partial t} = \nabla \cdot (c(\|\nabla I\|)\nabla I) \quad (1)$$

where  $\frac{\partial I}{\partial t}$  represents the change in pixel intensity over time.  $c(\|\nabla I\|)$  is the diffusion coefficient, which controls the amount of diffusion based on the gradient magnitude. The critical aspect of the PMD is the choice of diffusion  $c(\|\nabla I\|)$ . The two common forms of diffusion coefficients are exponential and inverse quadratic [31]. This study used the exponential form of (2).

$$c(\|\nabla I\|) = e^{-\left(\frac{\|\nabla I\|}{K}\right)^2} \quad (2)$$

where  $K$  is a parameter that controls the sensitivity of the diffusion process to edges. Small values of  $K$  result in more aggressive edge preservation, while larger values allow more smoothing. This iterative process is performed until a convergence condition is reached or a certain number of iterations is determined [32]. The edge-preserving property of the PMD filter comes from the behavior of the diffusion coefficient  $c(\|\nabla I\|)$ . Noise reduction is desired without blurring critical structural features, such as edges [33].

## 2.2. Contrast-limited adaptive histogram equalization

CLAHE is a popular image enhancement technique that improves local contrast by dividing an image into smaller regions (tiles) and applying HE to each tile independently. This approach enhances contrast in areas with different brightness levels. To prevent excessive amplification in uniform regions, CLAHE uses a limiting mechanism that preserves fine details while reducing artifacts [34]. The adjusted grayscale value  $K_i$  resulting from the histogram equalization process is computed using (3).

$$K_i = \text{round}\left(\frac{C_i(2^k - 1)}{w \cdot h}\right) \quad (3)$$

where  $C_i$  denotes the cumulative distribution function (CDF) of the  $i$ -th grayscale value in the original image,  $k$  represents the number of grayscale intensity levels, and  $w$  and  $h$  are the width and height of the image, respectively. In CLAHE, two main parameters govern the contrast quality of the resulting image: tile size and the clip limit. The tile size defines the dimensions of each sub-region, while the clip limit restricts the maximum slope of the CDF to avoid over-enhancement of noise. The clip limit  $\beta$  is defined as (4).

$$\beta = \frac{P}{Q} \left(1 + \frac{\alpha}{100} (S_{\max} - 1)\right) \quad (4)$$

where  $P$  is the tile area,  $Q$  is the total number of grayscale levels (typically 256),  $S_{\max}$  represents the maximum allowable slope in the CDF, and  $\alpha$  is the clip factor ranging from 0 to 100. This mechanism effectively reduces noise amplification and prevents the formation of artifacts in the enhanced image [35].

## 2.3. Spider monkey optimization

The SMO algorithm is a global optimization method inspired by the social behavior of spider monkeys during foraging and exploration. SMO seeks an optimal solution to complex optimization problems by mimicking spider monkeys' collaborative and adaptive behaviors [36]. In SMO, each spider monkey in a group is represented as  $SM_k (k = 1, 2, \dots, N)$ , serves as a potential solution. Each position vector of  $SM_k$  in a  $D$ -dimensional space represents possible solutions, initialized using (5).

$$SM_{k,j} = SM_{\min,j} + R (SM_{\max,j} - SM_{\min,j}) \quad (5)$$

$R$  is a random value between 0 and 1, and  $SM_{\max}$  and  $SM_{\min}$  upper and lower bounds are for each dimension. In the LL phase, each monkey's position is updated based on the local leader's guidance as in (6).

$$SM_{\text{new } i,j} = SM_{i,j} + R (Leader_{k,j} - SM_{i,j}) + U (SM_{r,j} - SM_{i,j}) \quad (6)$$

where  $Leader_{k,j}$  is the local leader,  $r$  is a randomly selected group member, and  $U$  is a uniform random variable in the range  $[-1, 1]$ . If the new position improves the solution, it is accepted; otherwise, it is discarded.

The global leadership (GL) phase updates positions based on global leader, where the probability  $prob_i$  is calculated using (7).

$$prob_i = 0.9 \times \frac{fit_i}{max_{fit}} + 0.1 \quad (7)$$

with the highest-fitness monkey serving as the global leader. After each iteration, leaders are updated through greedy selection in the L and GL phases. The local leader decision (LLD) phase prevents local leaders from stagnation by enforcing random position updates if a threshold (LocalLeaderLimit) is reached. Similarly, the global leader decision (GLD) phase splits the group if the GlobalLeaderLimit threshold is met, thus encouraging further exploration.

#### 2.4. Image quality assessment

IQA is the process of assessing or evaluating the quality of a digital image. Three IQA models can be used: reduced reference (RR-IQA), FR-IQA, and NR-IQA [37]. This study used MSE, SSIM, and PSNR to evaluate image denoising [38]. CEIQ, practical measure of EME, MC, RMS contrast, and entropy are also used to evaluate image contrast enhancement. EME is applied to quantify contrast-image enhancement, particularly for local contrast. It was calculated by dividing the image into blocks and considering the logarithmic ratio of the maximum and minimum intensities within each block.

$$EME = \frac{1}{M \times N} \sum_{i=1}^M \sum_{j=1}^N 20 \log \left( \frac{I_{max}(i,j)}{I_{min}(i,j)} \right) \quad (8)$$

$M$  and  $N$  are the number of blocks in the vertical and horizontal directions, respectively.  $(I_{max}(i,j))$  and  $(I_{min}(i,j))$  the maximum and minimum pixel intensities in the  $i$  and  $j$  block of the image. The logarithmic term helps measure contrast enhancement [39].

MC is a simple contrast measure defined as the difference between an image's maximum and minimum intensity, divided by their sum ( $I_{max}$ ) and ( $I_{min}$ ) are the image's maximum and minimum pixel intensity [39].

$$MC = \frac{I_{max} - I_{min}}{I_{max} + I_{min}} \quad (9)$$

The RMS contrast measures the overall contrast in an image by calculating the standard deviation of pixel intensities.  $I(i,j)$  is the intensity at the pixel location  $(i,j)$ .  $\bar{I}$  is the mean intensity of the entire image, and  $M$  and  $N$  are the image dimensions. The RMS contrast provides a single number that represents the contrast in an image, considering the variability in intensity values [39].

$$MS \text{ Contrast} = \sqrt{\frac{1}{MN} \sum_{i=1}^M \sum_{j=1}^N (I(i,j) - \bar{I})^2} \quad (10)$$

The entropy measures the amount of information or randomness in an image. It is often used to assess texture or complexity.

$$Entropy = \sum_{i=0}^{L-1} p_i \log_2(p_i) \quad (11)$$

$L$  is the total number of possible intensity levels.  $p_i$  is the probability (normalized histogram) of the occurrence of intensity level  $(i)$ . The entropy values range from 0 to  $\log_2(L)$ , with higher values indicating more complexity and randomness in the image [16].

The coefficient of correlation (CoC) measures the correlation between pixel intensities in an original image and a processed image. A high correlation indicates that the processed image retains the structural information of the original. CoC determines how well image enhancement preserves the original structural details as in (12).

$$CoC = \frac{\sum (I_x - \mu_x)(I_y - \mu_y)}{\sqrt{\sum (I_x - \mu_x)^2 \sum (I_y - \mu_y)^2}} \quad (12)$$

$I_x$  and  $I_y$  are pixel intensities in the original and enhanced images.  $\mu_x$  and  $\mu_y$  are mean intensities of the original and enhanced images.

Standard deviation (Std-dev) measures the spread of intensity values around the mean, reflecting the contrast variability in the image. Std-dev quantify intensity variation and contrast.

$$Std - dev = \sqrt{\frac{1}{N} \sum_{i=1}^N (I_i - \mu)^2} \quad (13)$$

$N$  is the total pixels in the image.  $I_i$  is the intensity of the  $i$ -th pixel.  $\mu$  is the mean intensity of the image.

## 2.5. Contrast enhancement-based image quality

CEIQ is an image quality assessment technique that leverages contrast enhancement for evaluation [26]. This method employs histogram equalization to analyze and quantify image contrast. This process involves dividing the image histogram into multiple bins and calculating the average intensity value for each bin. Subsequently, these average values assign new intensity values to pixels within each corresponding bin. Figure 2 shows the CEIQ evaluation model. CEIQ has two aspects of image quality assessment:

- The image similarity measures the similarity of the original image to that of the contrast-enhanced image. The image similarity was SSIM.
- Histogram entropy and cross-entropy measure an even distribution of the image histogram. The entropy ( $E$ ) equation is defined as (11). Cross-entropy ( $E_{xy}$ ) can be performed using the histogram equalization method. The cross-entropy values were calculated using (14).

$$E_{x,y} = -\sum_{i=0}^b h_x(i) \log h_y(i) \quad (14)$$

$h_x$  is the histogram of the original image and  $h_y$  the histogram of the contrast-enhanced image.

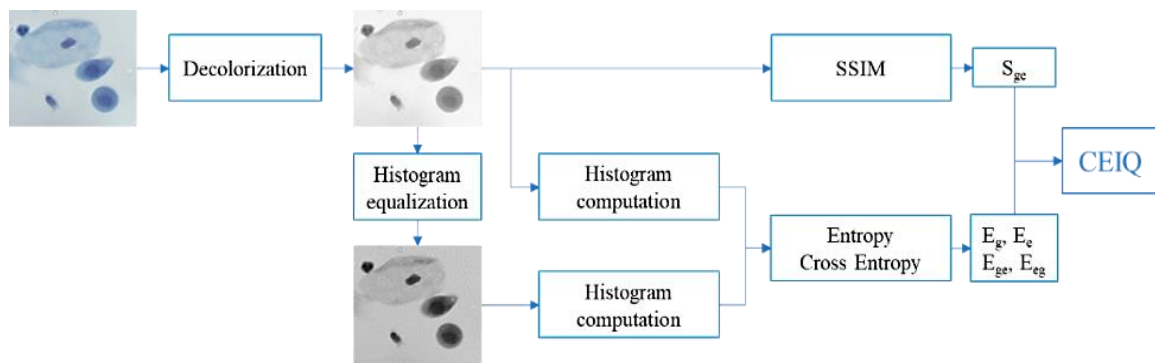


Figure 2. CEIQ evaluation model

## 2.6. Blind/reference-less image spatial quality evaluator

BRISQUE is a model that calculates features directly from image pixels, unlike other methods that rely on transformations to different spaces, such as wavelets or discrete cosine transformations (DCT). Its efficiency does not require these transformations to extract features. BRISQUE assesses the image quality by comparing the input image to a model trained on images with similar distortions. It is trained on a database of natural scene images with known distortions and incorporates subjective quality scores, making it opinion-aware. Lower BRISQUE values indicate better perceptual image quality [25].

## 3. RESULTS AND DISCUSSION

This section presents the performance results of the SMO-PMD filter, SMO-CLAHE, and hybrid optimization of the PMD filter and CLAHE with SMO, referred to as SMO-PMD-CLAHE. Each method was specifically optimized to improve image-quality metrics for effective noise reduction, improved contrast, and enhanced image clarity.

### 3.1. Spider monkey optimization-Perona-Malik diffusion filter

Table 1 shows the PMD filter optimization simulation results using PSO and SMO on ten images from SIPaKMeD. Overall, the SMO optimizer demonstrated superior performance across several key metrics

compared with the PSO optimizer. Regarding MSE, SMO achieved a lower average error of 0.0456 compared with 0.0572 for PSO, indicating that SMO is more effective in optimizing the PMD filter and minimizing the error between the original and denoised images. Similarly, SSIM is slightly higher for SMO (0.9984 compared to 0.9981 for PSO), suggesting that SMO produces images with structural quality that closely resemble the original images. Regarding PSNR, SMO again outperforms PSO in optimizing the PMD filter, with an average of 62.26 dB, indicating that SMO yields images with less noise, whereas PSO's average is 61.00 dB. Both methods exhibited nearly identical entropy values, indicating that the informational content and details within the images were well-preserved in both cases. In the BRISQUE score as an objective function, SMO produces a slightly lower value (36.8561) than PSO (37.3073), signifying that SMO provides a marginally better subjective visual quality.

Table 1. Result simulation in optimizing PMD filter using PSO and SMO

Images	Methods	MSE	SSIM	PSNR	Entropy	BRISQUE
013_02	PSO	0.043947645	0.996258439	61.70144756	4.571843131	0.686698775
	SMO	0.043389455	0.996305898	61.75696163	4.571857288	0.644838024
018_03	PSO	0.058383599	0.998492275	60.46789499	5.311107028	59.56556031
	SMO	0.025031866	0.999318272	64.14587134	5.311234326	57.95722145
019_01	PSO	0.126389165	0.996250434	57.11370518	5.498297928	54.46574524
	SMO	0.126785392	0.996229567	57.10011145	5.498286588	54.30521213
020_06	PSO	0.071592774	0.997519753	59.58211168	4.918457352	16.16094189
	SMO	0.071446865	0.99752755	59.59097187	4.918444596	16.14697568
023_01	PSO	0.053882471	0.998797808	60.81632858	5.705432895	82.87267047
	SMO	0.04483273	0.998983647	61.61485178	5.705490005	82.28349823
029_01	PSO	0.027944359	0.999283549	63.66786213	5.770480683	38.16081019
	SMO	0.026237661	0.999327682	63.94155247	5.770483568	38.09620783
039_01	PSO	0.035305231	0.99859665	62.65241301	5.430661391	33.79115112
	SMO	0.019000417	0.999242818	65.34317228	5.430631534	33.04454181
043_01	PSO	0.071355015	0.998425385	59.59655859	5.960775239	49.34384299
	SMO	0.039904779	0.999094202	62.12055451	5.96146055	48.20374569
048_01	PSO	0.056730497	0.999230125	60.59263776	6.316787802	34.89882012
	SMO	0.035746326	0.999523087	62.59848949	6.316873752	34.85028191
050_06	PSO	0.026868811	0.998198142	63.83831907	4.766578449	3.126566942
	SMO	0.023824182	0.998404514	64.36062355	4.766553067	3.028702503
Average	PSO	0.057239957	0.998105256	61.00292786	5.42504219	37.3072808
	SMO	0.045619967	0.998395724	62.25731604	5.425131527	36.85612253

These results suggest that SMO generally delivers a better image quality than PSO when optimizing the PMD filter. SMO consistently outperforms PSO in critical metrics, such as MSE, SSIM, PSNR, and BRISQUE. SMO-PMD filter offers new insight for applications requiring high image processing accuracy. Although the entropy values are similar between the two methods, SMO's consistent superiority in reducing error and noise.

### 3.2. Spider monkey optimization-contrast-limited adaptive histogram equalization

The simulation results for CLAHE optimization using the POA and SMO algorithms on 10 images from the SIPaKMeD dataset can be seen in Figure 3. These results show relatively small differences across key metrics such as entropy, EME, RMS contrast, CoC, Std-dev, CEIQ, and processing time. Regarding entropy, the results were almost identical for both methods across all images, suggesting that the POA and SMO maintained similar levels of pixel intensity information. A similar trend is observed in the EME and RMS contrasts, where there is no significant difference between the two methods, indicating that both handle contrast enhancement similarly.

One of the primary differences between the two methods is the processing time. SMO consistently outperformed POA in terms of speed. The average processing time for SMO was 7.5470 s, compared with 7.7650 s. This highlights the efficiency of SMO in terms of computational time, making it preferable in scenarios in which rapid image processing is essential, particularly for large-scale image datasets. The simulation results provide valuable insights into the performance of the POA and SMO in optimizing CLAHE on cervical images. Both methods showed comparable results in maintaining the image quality, as reflected in the near-identical values of entropy, EME, and RMS contrast. These metrics confirm that both POA and SMO can effectively enhance the contrast without significant loss of information. However, for practical implementation, processing time is a crucial factor. Therefore, SMO-CLAHE was more effective for cervical cancer detection.

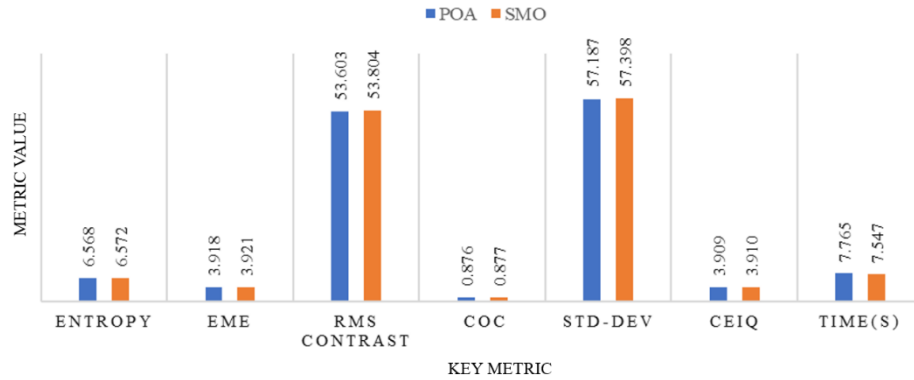


Figure 3. Average results of CLAHE optimization using POA and SMO

### 3.2.1. Hybrid SMO PMD-CLAHE

The average results for each evaluation metric on 10 cervical images using the SMO-PMD, SMO-CLAHE, and hybrid SMO PMD-CLAHE algorithms can be seen in Figure 4. The metrics used in this evaluation are EME, MC, RMS contrast, entropy, and CEIQ. The SMO PMD method achieved the lowest EME value of 1.23, indicating limited effectiveness in enhancing illumination quality. SMO CLAHE demonstrated a significant improvement with an EME value of 3.85, while the combination of SMO PMD-CLAHE achieved the highest value of 5.45. This confirms that combining PMD and CLAHE has a synergistic effect, resulting in images with superior illumination quality. For Michelson contrast, SMO PMD and SMO PMD-CLAHE achieved nearly optimal values of 1.00 and 0.99, respectively, indicating excellent contrast distribution. On the other hand, SMO CLAHE produced a lower MC value of 0.85, indicating slightly reduced contrast compared to the different methods.

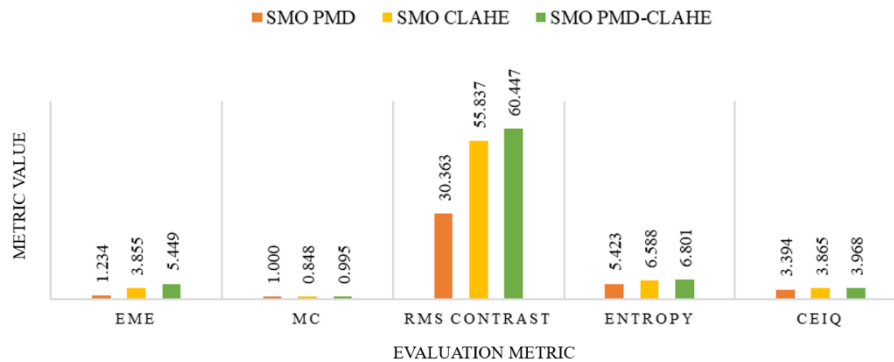


Figure 4. The average result on PMD, CLAHE, and Hybrid PMD-CLAHE optimization using SMO

The SMO PMD method had the lowest RMS contrast value of 30.36, suggesting limited enhancement capability. In contrast, SMO CLAHE showed a significant improvement with a value of 55.83, while SMO PMD-CLAHE achieved the highest value of 60.45. This demonstrates that combining PMD and CLAHE provides richer and more optimal contrast in the resulting images. The entropy values reflect the diversity of information in the images. SMO PMD recorded the lowest value of 5.42, indicating less detailed images. SMO CLAHE achieved a higher entropy value of 6.59. At the same time, the combination of SMO PMD-CLAHE excelled with the highest entropy value of 6.80, indicating that this method produced images with the richest information details. Regarding CEIQ, SMO PMD had the lowest value of 3.39, indicating suboptimal enhancement of contrast quality. SMO CLAHE achieved a higher CEIQ value of 3.87, while the combination of SMO PMD-CLAHE delivered the best results with a CEIQ value of 3.97.

The results demonstrate that the combination of SMO PMD-CLAHE delivers the best performance across almost all evaluation metrics. This combination effectively improves illumination, contrast, and image information details. It outperforms both SMO PMD and SMO CLAHE when applied individually. In medical image analysis, optimal image quality is crucial for supporting more accurate diagnostic processes,



particularly for pap-smear images. Therefore, the SMO PMD-CLAHE combination is recommended to enhance overall image quality. This approach can potentially be applied to other scenarios in medical image processing, where improving image quality plays a vital role in supporting clinical decision-making.

#### 4. CONCLUSION

This study presents a practical noise-reduction and contrast-enhancement framework for pap-smear images. The proposed method thoroughly evaluates image quality improvement by focusing on clarity, detail preservation, and contrast enhancement. A hybrid PMD-CLAHE method was optimized using the SMO algorithm to overcome the common problems of noise and low contrast in the pap-smear images. The hybrid SMO-PMD-CLAHE leverages the noise reduction capabilities of the PMD filter while maximizing contrast enhancement through CLAHE. The SMO algorithm consistently provides superior results in optimizing the PMD filter and CLAHE compared with the PSO and POA algorithms. BRISQUE is introduced as a new objective function for PMD filter optimization. BRISQUE performs significantly better than traditional metrics, such as PSNR and SSIM. Similarly, CEIQ is used as a new objective function for CLAHE optimization. CEIQ is a comprehensive assessment of contrast enhancement using a combination of entropy, cross-entropy, and SSIM. The SMO-PMD-CLAHE hybrid approach achieved the highest performance across all evaluated metrics compared with SMO-PMD or SMO-CLAHE. The proposed method, SMO PMD-CLAHE, significantly improved the pap-smear image quality with noise reduction and contrast enhancement.

#### FUNDING INFORMATION

This research was financially supported by the Ministry of Higher Education, Science, and Technology of the Republic of Indonesia in collaboration with the Indonesian Endowment Fund for Education (LPDP). The funding was provided through the Indonesian Education Scholarship (BPI) program, which is administered by the Center for Higher Education Funding and Assessment (PPAPT). BPI ID: 202327091034.

#### AUTHOR CONTRIBUTIONS STATEMENT

This journal uses the Contributor Roles Taxonomy (CRediT) to recognize individual author contributions, reduce authorship disputes, and facilitate collaboration.

Name of Author	C	M	So	Va	Fo	I	R	D	O	E	Vi	Su	P	Fu
Ach Khozaimi	✓	✓	✓		✓			✓	✓		✓		✓	✓
Isnani Darti	✓	✓	✓			✓	✓	✓		✓	✓	✓		
Wuryansari Muharini	✓	✓		✓		✓				✓		✓	✓	
Kusumawinahyu														
Syaiful Anam		✓		✓	✓		✓			✓		✓		

C : **C**onceptualization

M : **M**ethodology

So : **S**oftware

Va : **V**alidation

Fo : **F**ormal analysis

I : **I**nvestigation

R : **R**esources

D : **D**ata Curation

O : Writing - **O**riginal Draft

E : Writing - Review & **E**diting

Vi : **V**isualization

Su : **S**upervision

P : **P**roject administration

Fu : **F**unding acquisition

#### CONFLICT OF INTEREST STATEMENT

The authors declare that there is no conflict of interest regarding the publication of this paper.

#### DATA AVAILABILITY

The SIPaKMeD dataset utilized in this study is available at <https://bit.ly/SIPaKMeD>.

#### REFERENCES

- [1] G. Curigliano *et al.*, "Management of cardiac disease in cancer patients throughout oncological treatment: esmo consensus recommendations," *Annals of Oncology*, vol. 31, no. 2, pp. 171–190, Feb. 2020, doi: 10.1016/j.annonc.2019.10.023.
- [2] B. A. Tjokroprawiro, K. Novitasari, W. Saraswati, I. Yuliati, R. A. Ulhaq, and H. A. Sulistya, "The challenging journey of cervical cancer diagnosis and treatment at the second largest hospital in indonesia," *Gynecologic Oncology Reports*, vol. 51, Feb. 2024, doi: 10.1016/j.gore.2024.101325.




*Optimized pap-smear image enhancement: hybrid Perona-Malik diffusion filter-CLAHE ... (Ach Khozaimi)*

- [3] D. Sambyal and A. Sarwar, "Recent developments in cervical cancer diagnosis using deep learning on whole slide images: an overview of models, techniques, challenges and future directions," *Micron*, vol. 173, Oct. 2023, doi: 10.1016/j.micron.2023.103520.
- [4] A. D. Jia, B. Zhengyi Li, and C. C. Zhang, "Detection of cervical cancer cells based on strong feature CNN-SVM network," *Neurocomputing*, vol. 411, pp. 112–127, Oct. 2020, doi: 10.1016/j.neucom.2020.06.006.
- [5] L. Allahqoli *et al.*, "Diagnosis of cervical cancer and pre-cancerous lesions by artificial intelligence: a systematic review," *Diagnostics*, vol. 12, no. 11, Nov. 2022, doi: 10.3390/diagnostics12112771.
- [6] M. Zhao *et al.*, "SEENS: nuclei segmentation in pap smear images with selective edge enhancement," *Future Generation Computer Systems*, vol. 114, pp. 185–194, Jan. 2021, doi: 10.1016/j.future.2020.07.045.
- [7] V. Kamalaveni, R. A. Rajalakshmi, and K. A. Narayanankutty, "Image denoising using variations of Perona-Malik model with different edge stopping functions," *Procedia Computer Science*, vol. 58, pp. 673–682, 2015, doi: 10.1016/j.procs.2015.08.087.
- [8] S. Anam, Z. Fitriah, and N. Shofianah, "Hybrid of the PMD filter, the k-means clustering method and the level set method for exudates segmentation," in *Proceedings of the International Conference on Mathematics and Islam*, SCITEPRESS-Science and Technology Publications, 2018, pp. 108–116, doi: 10.5220/0008517901080116.
- [9] S. V. Ezhilramana, "Bilateral Perona-Malik diffusion filtering based topological multitude feature vector for breast cancer detection," *Journal of Research on the Lepidoptera*, vol. 51, no. 1, pp. 110–128, Feb. 2020, doi: 10.36872/LEPI/V51I1/301010.
- [10] M. M. Rahaman *et al.*, "A survey for cervical cytopathology image analysis using deep learning," *IEEE Access*, vol. 8, pp. 61687–61710, 2020, doi: 10.1109/ACCESS.2020.2983186.
- [11] C. Tsotsios and M. Petrou, "On the choice of the parameters for anisotropic diffusion in image processing," *Pattern Recognition*, vol. 46, no. 5, pp. 1369–1381, May 2013, doi: 10.1016/j.patcog.2012.11.012.
- [12] A. Jeelani and M. B. Veena, "Hybridization of PSO and anisotropic diffusion in denoising the images," in *Microelectronics, Electromagnetics and Telecommunications*, Springer, Singapore, 2018, pp. 463–473, doi: 10.1007/978-981-10-7329-8\_47.
- [13] E. A. Tjoa, I. P. Y. N. Suparta, R. Magdalena, and N. K. CP, "The use of clahe for improving an accuracy of CNN architecture for detecting pneumonia," *SHS Web of Conferences*, vol. 139, May 2022, doi: 10.1051/shsconf/202213903026.
- [14] M. Hayati *et al.*, "Impact of CLAHE-based image enhancement for diabetic retinopathy classification through deep learning," *Procedia Computer Science*, vol. 216, pp. 57–66, 2023, doi: 10.1016/j.procs.2022.12.111.
- [15] A. Desiani, Erwin, B. Suprihatin, S. Yahdin, A. I. Putri, and F. R. Husein, "Bi-path architecture of CNN segmentation and classification method for cervical cancer disorders based on pap-smear images," *IAENG International Journal of Computer Science*, vol. 48, no. 3, 2021.
- [16] H. M. Qassim, N. M. Basheer, and M. N. Farhan, "Brightness preserving enhancement for dental digital x-ray images based on entropy and histogram analysis," *Journal of Applied Science and Engineering*, vol. 22, no. 1, pp. 187–194, 2019, doi: 10.6180/jase.201903\_22(1).0019.
- [17] L. G. More, M. A. Brizuela, H. L. Ayala, D. P. Pinto-Roa, and J. L. V. Noguera, "Parameter tuning of CLAHE based on multi-objective optimization to achieve different contrast levels in medical images," in *2015 IEEE International Conference on Image Processing (ICIP)*, IEEE, Sep. 2015, pp. 4644–4648, doi: 10.1109/ICIP.2015.7351687.
- [18] A. Fawzi, A. Achuthan, and B. Belaton, "Adaptive clip limit tile size histogram equalization for non-homogenized intensity images," *IEEE Access*, vol. 9, pp. 164466–164492, 2021, doi: 10.1109/ACCESS.2021.3134170.
- [19] U. Kuran and E. C. Kuran, "Parameter selection for clahe using multi-objective cuckoo search algorithm for image contrast enhancement," *Intelligent Systems with Applications*, vol. 12, Nov. 2021, doi: 10.1016/j.iswa.2021.200051.
- [20] U. Kuran, E. C. Kuran, and M. B. Er, "Parameter selection of contrast limited adaptive histogram equalization using multi-objective flower pollination algorithm," in *Electrical and Computer Engineering (ICECENG 2022)*, Springer, Cham, 2022, pp. 109–123, doi: 10.1007/978-3-031-01984-5\_9.
- [21] S. Surya and A. Muthukumaravel, "Adaptive sailfish optimization-contrast limited adaptive histogram equalization (ASFO-CLAHE) for hyperparameter tuning in image enhancement," in *Computational Intelligence for Clinical Diagnosis*, Springer, Cham, 2023, pp. 57–76, doi: 10.1007/978-3-031-23683-9\_5.
- [22] S. R. Borra, N. P. Tejaswini, V. Malathy, B. M. Kumar, and M. I. Habelalmateen, "Contrast limited adaptive histogram equalization based multi-objective improved cat swarm optimization for image contrast enhancement," in *2023 International Conference on Integrated Intelligence and Communication Systems (ICIICS)*, IEEE, 2023, pp. 1–5, doi: 10.1109/ICIICS59993.2023.10420959.
- [23] Y. R. Haddadi, B. Mansouri, and F. Z. I. Khodja, "A novel medical image enhancement algorithm based on clahe and pelican optimization," *Multimedia Tools and Applications*, vol. 83, no. 42, pp. 90069–90088, 2024, doi: 10.1007/s11042-024-19070-6.
- [24] H. Zhu, Y. Wang, Z. Ma, and X. Li, "A comparative study of swarm intelligence algorithms for UCAV path-planning problems," *Mathematics*, vol. 9, no. 2, Jan. 2021, doi: 10.3390/math9020171.
- [25] A. Mittal, A. K. Moorthy, and A. C. Bovik, "No-reference image quality assessment in the spatial domain," *IEEE Transactions on Image Processing*, vol. 21, no. 12, pp. 4695–4708, Dec. 2012, doi: 10.1109/TIP.2012.2214050.
- [26] J. Yan, J. Li, and X. Fu, "No-reference quality assessment of contrast-distorted images using contrast enhancement," *arXiv-Computer Science*, pp. 1–15, Apr. 2019.
- [27] R. Kumar and A. K. Bhandari, "Noise reduction deep CNN-based retinal fundus image enhancement using recursive histogram," *Neural Computing and Applications*, vol. 36, no. 27, pp. 17221–17243, 2024, doi: 10.1007/s00521-024-09996-1.
- [28] K. P. Win, Y. Kitjaidure, K. Hamamoto, and T. Myo Aung, "Computer-assisted screening for cervical cancer using digital image processing of pap smear images," *Applied Sciences*, vol. 10, no. 5, Mar. 2020, doi: 10.3390/app10051800.
- [29] M. E. Plissiti, P. Dimitrakopoulos, G. Sfikas, C. Nikou, O. Krikoni, and A. Charchanti, "Sipakmed: a new dataset for feature and image based classification of normal and pathological cervical cells in pap smear images," in *2018 25th IEEE International Conference on Image Processing (ICIP)*, IEEE, Oct. 2018, pp. 3144–3148, doi: 10.1109/ICIP.2018.8451588.
- [30] S. Ray, K. G. Dhal, and P. K. Naskar, "Particle swarm optimizer based epithelial layer segmentation in CIElab color space," in *2022 IEEE 7th International Conference on Recent Advances and Innovations in Engineering (ICRAIE)*, IEEE, Dec. 2022, pp. 331–336, doi: 10.1109/ICRAIE56454.2022.10054261.
- [31] P. Perona and J. Malik, "Scale-space and edge detection using anisotropic diffusion," *IEEE Transactions on Pattern Analysis and Machine Intelligence*, vol. 12, no. 7, pp. 629–639, Jul. 1990, doi: 10.1109/34.56205.
- [32] A. V. Nasonov, N. V. Mamaev, O. S. Volodina, and A. S. Krylov, "Automatic choice of denoising parameter in Perona-Malik model," in *29th International Conference on Computer Graphics, Image Processing and Computer Vision, Visualization Systems and the Virtual Environment GraphiCon'2019*, Nov. 2019, pp. 144–147, doi: 10.30987/graphicon-2019-2-144-147.
- [33] B. Maiseli, "Nonlinear anisotropic diffusion methods for image denoising problems: challenges and future research opportunities," *Array*, vol. 17, Mar. 2023, doi: 10.1016/j.array.2022.100265.




- [34] S. Muniyappan, A. Allirani, and S. Saraswathi, "A novel approach for image enhancement by using contrast limited adaptive histogram equalization method," in *2013 Fourth International Conference on Computing, Communications and Networking Technologies (ICCCNT)*, IEEE, Jul. 2013, pp. 1–6, doi: 10.1109/ICCCNT.2013.6726470.
- [35] M. Widyaningsih, T. K. Priyambodo, M. E. Wibowo, and M. Kamal, "Optimization contrast enhancement and noise reduction for semantic segmentation of oil palm aerial imagery," *International Journal of Intelligent Engineering and Systems*, vol. 16, no. 1, pp. 597–609, Feb. 2023, doi: 10.22266/ijies2023.0228.51.
- [36] J. C. Bansal, H. Sharma, S. S. Jadon, and M. Clerc, "Spider monkey optimization algorithm for numerical optimization," *Memetic Computing*, vol. 6, no. 1, pp. 31–47, Mar. 2014, doi: 10.1007/s12293-013-0128-0.
- [37] V. Kamble and K. M. Bhurchandi, "No-reference image quality assessment algorithms: a survey," *Optik*, vol. 126, no. 11–12, pp. 1090–1097, Jun. 2015, doi: 10.1016/j.ijleo.2015.02.093.
- [38] U. Sara, M. Akter, and M. S. Uddin, "Image quality assessment through FSIM, SSIM, MSE and PSNR—a comparative study," *Journal of Computer and Communications*, vol. 07, no. 03, pp. 8–18, 2019, doi: 10.4236/jcc.2019.73002.
- [39] C. Avatavulvi and M. Prodan, "Evaluating image contrast: a comprehensive review and comparison of metrics," *Journal of Information Systems & Operations Management*, vol. 17, no. 1, 2023.

## BIOGRAPHIES OF AUTHORS






**Ach Khozaimi**    is a lecturer in Informatics Engineering at Trunojoyo University of Madura, Indonesia. He earned his bachelor's degree in Informatics from Trunojoyo University of Madura and his master's degree in Informatics from Institut Teknologi Sepuluh Nopember (ITS), Indonesia. Currently, he is pursuing a Ph.D. in the Department of Mathematics at Brawijaya University, Indonesia. His doctoral studies are funded by the Center for Higher Education Funding and Assessment (PPAPT) under the Ministry of Higher Education, Science, and Technology of the Republic of Indonesia. He can be contacted at email: khozaimi@trunojoyo.ac.id.






**Isnani Darti**    stands as the 24th active Professor at the Faculty of Mathematics and Natural Sciences (FMIPA) and the 176th active at the university overall. Her research interests span several captivating domains: applied dynamical systems, mathematical biology, optical solitons, and discretization of continuous dynamical systems. Recently, she achieved the prestigious rank of Professor at Brawijaya University. Her professorship adds to the rich legacy of Brawijaya University, where she is the 335th Professor in its history. She can be contacted at email: isnanidarti@ub.ac.id.



**Wuryansari Muharini Kusumawinahyu**    received her Doctoral Degree in Mathematics from Institut Teknologi Bandung (ITB), Indonesia in 2006. She also earned her Bachelor's Degree in Mathematics from ITB in 1991 and her Master's Degree from the same institution in 1995. She is currently an associate professor at the Department of Mathematics, Faculty of Science, Universitas Brawijaya, Malang, Indonesia. Her research includes mathematical epidemiology, predator-prey models, and wave dynamics. She has published numerous papers in national and international journals. She can be contacted at email: wmuharini@ub.ac.id.



**Syaiful Anam**    received a Doctor of Natural Science and Mathematics degree from Yamaguchi University, Japan in 2015. He also received his Bachelor's Degree in Mathematics from Brawijaya University, Indonesia in 2001 and his Master Degree from Sepuluh Nopember Institute of Technology, Indonesia in 2006. He is currently an assistant professor at Department of Mathematics, Brawijaya University, Malang, Indonesia. His research includes data science, computational intelligence, machine learning, digital image processing, and computer vision. He has published over 35 papers in international journals and conferences. He can be contacted at email: syaiful@ub.ac.id.